Josephson amplifier for qubit readout

Baleegh Abdo, Flavius Schackert, Michael Hatridge, Chad Rigetti, and Michel Devoret

Related Articles

Superconducting low-inductance undulatory galvanometer microwave amplifier
Appl. Phys. Lett. 100, 063503 (2012)

Current states of a doubly connected superconductor with two point contacts
Low Temp. Phys. 38, 35 (2012)

Strain enhanced electron cooling in a degenerately doped semiconductor
Appl. Phys. Lett. 99, 251908 (2011)

Superconducting qubits consisting of epitaxially grown NbN/AlN/NbN Josephson junctions
Appl. Phys. Lett. 99, 212502 (2011)

Current amplification with vertical Josephson interferometers
J. Appl. Phys. 110, 073910 (2011)

Additional information on Appl. Phys. Lett.

Journal Homepage: http://apl.aip.org/

Journal Information: http://apl.aip.org/about/about_the_journal

Top downloads: http://apl.aip.org/features/most_downloaded

Information for Authors: http://apl.aip.org/authors
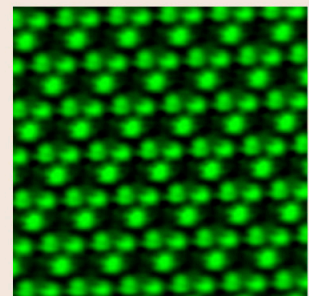
Josephson amplifier for qubit readout

Baleegh Abdo, Flavius Schackert, Michael Hatridge, Chad Rigetti,[a)] and Michel Devoret[b)]
Department of Applied Physics, Yale University, New Haven, Connecticut 06520, USA

We report on measurements of a Josephson amplifier (J-amp) suitable for quantum-state qubit readout in the microwave domain. It consists of two microstrip resonators which intersect at a Josephson ring modulator. A maximum gain of about 20 dB, a bandwidth of 9 MHz, and a center-frequency tunability of about 60 MHz with gain in excess of 10 dB have been attained for idler and signal of frequencies 6.4 GHz and 8.1 GHz, in accordance with theory. Maximum input power measurements of the J-amp show a relatively good agreement with theoretical prediction. We discuss how the amplifier characteristics can be improved. © 2011 American Institute of Physics. [doi:10.1063/1.3653473]

One of the major hurdles which scientists confront in the growing area of solid state quantum information systems is the relatively high noise temperature of commercial amplifiers in the microwave domain[1] based on high electron mobility transistors (HEMTs), which have a noise temperature above 2 K. In order to overcome this pressing problem several low-noise amplification schemes have been utilized, such as the use of rf-SETs,[2,3] dc-SQUIDs,[4–6] nanoSQUIDs,[7] and flux qubits.[8] In addition, amplification schemes which employ large unshunted Josephson tunnel junctions[9–14] have appeared recently very promising, especially two main device variations, namely the degenerate parametric amplifier[15–17] and the non-degenerate parametric amplifier.[18,19]

Both parametric amplifiers, the degenerate and the non-degenerate, can be operated in either phase sensitive amplification mode where they amplify only one quadrature of the microwave field without adding noise to the processed signal, or in phase preserving amplification mode where they amplify both quadratures of the microwave field at the expense of adding at least a noise equivalent to a half input photon at the signal frequency.[18,20] However, only the non-degenerate amplifier has the advantage of a full pump-signal separation in the phase preserving mode.

In a previous work by our group Bergeal *et al.*[18] have demonstrated a proof of principle device based on Josephson junctions and coplanar waveguide resonators which performs a full non-degenerate three-wave mixing amplification of microwave signals. The device was named the Josephson parametric converter (JPC) in order to emphasize its unique frequency conversion property compared to other degenerate amplifiers. As a preamplifier preceding the HEMT, the JPC had two important characteristics: it achieved gains in excess of 40 dB and operated near the quantum limit. In the present work we report new results of a practical and well controlled Josephson amplifier (J-amp) based on the JPC, which is suitable for qubit readout. To that end, the main advantage of the present device is that it attains a high gain-bandwidth product $(\sqrt{G}B)$ of 0.1 GHz, where G is the power gain of the

device and B is the 3 dB bandwidth at gain G. While a 20 dB of gain is required in order to beat the noise floor of the following amplifier, a large bandwidth of the order of 10 MHz is essential in order to process input signals on a time scale less than 100 ns.

The J-amp consists of two half-wave microstrip resonators denoted as signal (S) and idler (I) which intersect at an rf-current anti-node of the resonators where a Josephson ring modulator (JRM) is incorporated. The latter element consists of four Josephson junctions arranged in a Wheatstone bridge configuration with half a flux quantum threading the ring (see Fig. 1). Both S and I are the differential eigenmodes of the JRM system.[19,21] The two resonators supporting these modes shown in Fig. 1 have a loaded resonance frequency $f_S^{res} = 8.11$ GHz and $f_I^{res} = 6.44$ GHz, a loaded quality factor $Q_S = 100$ and $Q_I = 64$ corresponding to bandwidths $\kappa_S/2\pi = 81$ MHz and $\kappa_I/2\pi = 100$ MHz respectively.

When operated as an amplifier, the device mixes two incoming low intensity fields, i.e., the signal and the idler having frequencies f_S and f_I, with an intense microwave field
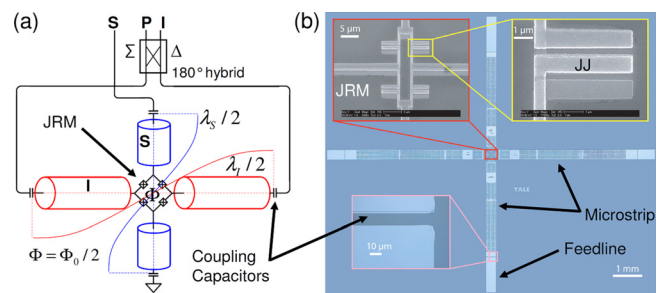

FIG. 1. (Color online) (a) A circuit representation of the J-amp device based on the JPC consisting of two half-wave transmission line resonators ($\lambda_S/2$ and $\lambda_I/2$) supporting two eigenmodes of the JRM, denoted as signal (S) and idler (I). The idler is fed through the difference port (Δ) of a 180° hybrid, while the third eigenmode denoted as pump (P) is non-resonant and fed to the device via the sum port (Σ). The flux bias applied to the ring is half a flux-quantum. (b) Optical microscope image of the J-amp device, consisting of two microstrip resonators and a JRM at the middle. The upper insets show zoom-in SEM micrographs of the JRM (left inset) and one Josephson junction of the ring (right inset). The bottom inset shows one of the gap capacitors which couple the feedlines to the resonators and determine the total quality factor of the resonators.

a)Current address: IBM T. J. Watson Research Center, Yorktown Heights, New York 10598, USA.
b)Electronic mail: michel.devoret@yale.edu.

called pump (P) having a frequency $f_P = f_S + f_I$ and applied using the common mode of the JRM.

The measurements presented in this paper were carried out in a cryogen-free dilution fridge at 30 mK. The experimental scheme used is similar to that employed in previous experiments.[18] It consists of five lines, two for each of the idler and the signal modes serving as input and output, where both input and output lines are connected to the sample through a cryogenic circulator at base temperature. The fifth line carries the pump signal P. The input lines include cryogenic attenuators at the 4 K stage and base, while the output lines include base temperature circulators, a cryogenic HEMT amplifier at the 4 K stage and an additional amplification stage at room temperature. A small magnetic coil positioned on top of the sample mount was used to flux bias the JRM loop at the amplification working point $\varphi \approx \varphi_0/2$, where $\varphi_0 = \hbar/2e$. Note that both P and I in the present design are fed to the resonator of the J-amp via a 180° hybrid as shown in Fig. 1(a) and not through direct capacitive coupling to the JRM as in Ref. 18. This new method simplifies the design considerably as it cancels the need of an on-chip wire cross-over.

The J-amp sample was fabricated on a 300 μm thick silicon chip having a resistivity larger than $1\,\mathrm{k\Omega} \times \mathrm{cm}$. An optical microscope image of the J-amp as well as SEM micrographs of the JRM and one of the Josephson junctions are shown in Fig. 1(b). The microstrip resonators and the JRM are made of aluminum. The entire chip was written using a one-layer e-beam lithography process. The Al/AlO$_x$/Al Josephson junctions were evaporated using a standard shadow mask evaporation process. The Josephson junction area is $5\,\mu\mathrm{m} \times 1\,\mu\mathrm{m}$, while the loop area of the JRM is about $50\,\mu\mathrm{m}^2$. The critical current of the nominally identical Josephson junctions of the JRM is $I_0 = 3 \pm 0.5\,\mu\mathrm{A}$. The spider-web-like structure of the top conductor of the microstrip resonators was utilized in order to reduce potential losses due to vortex motion.

In Fig. 2 we plot amplification curves of the signal as a function of frequency measured in reflection. The gain curves shown in the figure correspond to different pump frequencies as listed in the legend, where for each applied pump frequency the pump power was adjusted to yield maximum gain. The figure shows a maximum signal gain of about 18 dB and a center-frequency tunability of about 60 MHz with gain in excess of 10 dB in agreement with theory. Furthermore, due to a good bandwidth matching between S and I resonators, similar frequency tunability was achieved for the idler as well.

The interplay between G and B of the device is shown in Fig. 3. According to J-amp theory,[19,21] in the limit of large gains ($G \gg 1$) the amplification bandwidth (corresponding to the -3 dB points below the maximum) varies with the device gain as $B = 2(2\pi/\kappa_I + 2\pi/\kappa_S)^{-1}G^{-1/2}$. In Fig. 3 the measured bandwidth of the J-amp at resonant tuning ($f_P = f_S^{res} + f_I^{res}$) is plotted versus $G^{-1/2}$ for both the signal (blue circles) and the idler (red squares). The blue and red dashed lines are linear fits to the data, and they coincide to a good agreement with the theoretical prediction for large gains (drawn as a solid black line) and also extrapolate well to the bare bandwidths measured for the signal and idler resonators at $\varphi = \varphi_0/2$ with no gain (pump off). At the maximum-gain points in the figure (expressed in linear scale), the J-amp attains 19.1 dB of gain and 11.3 MHz of bandwidth for the signal mode and 20.7 dB and 9.4 MHz for the idler mode.

Moreover, by measuring the improvement in the signal to noise ratio of the system due to the presence of the J-amp and the noise temperature of the output lines, we are able to set an upper limit on the amount of noise added by the J-amp to the input which was found to be 1 ± 0.5 photon at the signal frequency.

Another important figure of merit of the device is the 1 dB compression point, i.e., the maximum signal power at the input of the device, denoted as P_{max}, at which the gain of the device drops by 1 dB below G_0 (the gain of the device for a vanishing input power). In Fig. 4 we plot the signal gain as a function signal power. The different data sets correspond to different values of G_0. The 1 dB compression point of each data set is indicated in green. The dashed green line connecting these points is a guide for the eye. The solid red curve corresponds to a Microwave Office simulation of the J-amp based on a transmission-line-model.[19,21]

The theoretical bound on the maximum signal power of the J-amp derived in Ref. 21 $P_{max} = (0.16\pi/p_Sp_IQ_SQ_I)(\gamma_P\omega_S/\omega_P^2)(Z_0I_0^2/(G_0 - 1))$ is shown in Fig. 4 as a black
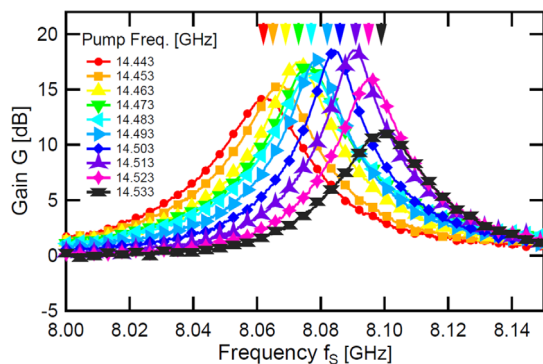

FIG. 2. (Color online) Gain curves of the signal mode versus frequency. The center frequency of the amplifier is tuned by varying the pump frequency. The data show a frequency range of about 60 MHz in which the signal gain exceeds 10 dB. The arrows plotted on top of the curves indicate the locations of the calculated signal frequencies.
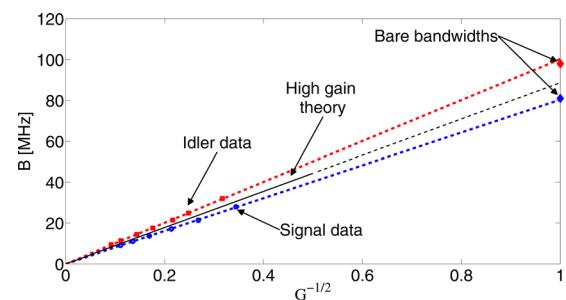

FIG. 3. (Color online) The bandwidth of the amplifier B versus $1/\sqrt{G}$. The red (squares) and blue (circles) correspond to idler and signal data respectively. The linear fits drawn as red and blue dashed lines satisfy a relation of the form $B\sqrt{G} = const$. The black solid line depicts the theoretical expression for the bandwidth B of the amplifier in the high gain limit (see text). The two diamond-shaped points red (top) and blue (bottom) drawn at unity gain correspond to the bandwidths of the bare resonators I and S, respectively.
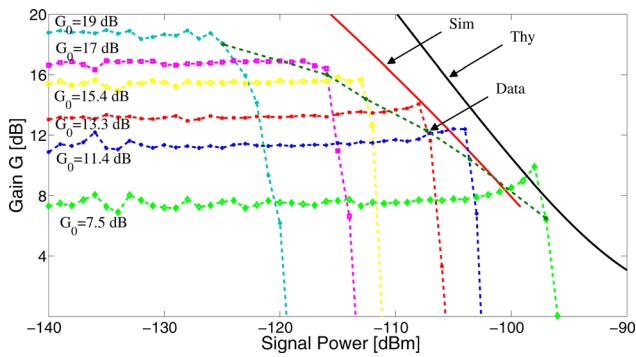
FIG. 4. (Color online) A 1 dB compression point measurement of the J-amp as a function of signal gain. The dashed green line connects 1 dB compression points measured for different gains G_0. The black curve depicts the upper limit on the signal power predicted by theory. The solid red curve corresponds to a Microwave Office transmission-line simulation of the device in the range of measured gains.

curve, where ω_S and ω_P are the angular frequencies of the signal and the pump, $p_{S,I} = L_J/(L_J + L_{S,I}) \simeq 0.03 - 0.04$ is the participation ratio of the device,[19,21] where L_J is the effective Josephson junction inductance at the working point given by $L_J = \sqrt{2}\varphi_0/I_0$ and $L_{S,I}$ is the effective inductance of the S and I resonators, $\gamma_P/2\pi \simeq 0.9$ GHz is the residence rate of photons at ω_P and $Z_0 = 50\,\Omega$ is the characteristic impedance of the feedline.

By comparing the dashed green line and the solid black or red curves, we see that in the low gain limit both theory and simulation curves show a good agreement with the data. However, in the high gain limit the slope of the decrease in P_{max} as a function of G_0 becomes larger than ~ -1 dB/dB predicted by theory or ~ -1.3 dB/dB given by simulation. An important key to understanding this discrepancy is the behavior of the gain in the vicinity of P_{max}. Steep drops in the gain similar to the ones seen in Fig. 4 suggest that the device enters a chaotic regime at P_{max} due to nonlinear processes taking place in the Josephson junctions which are not accounted for in the simplified ideal theoretical expression or in the simulation. Other devices, where the pQ product was increased at the expense of the gain-bandwidth product, exhibited a qualitatively different behavior near P_{max}. In these devices, the drop in gain is gradual and the gain curves are in full agreement with theory and simulation.

It is worthwhile noting that P_{max} which can be processed by the present device at 19 dB of gain is -125 dBm, which corresponds to 5 photons at the signal frequency times the amplifier dynamic bandwidth. Thus, allowing for qubit state readout which is performed, in general, using one photon on average in the readout cavity with a bandwidth of 20 MHz (Ref. 22).

In order to enhance the P_{max} figure of the device while maintaining the current values for G, ω, and B, I_0 should be increased according to the theoretical expression. However, such increase in I_0 implies decreasing $L_{S,I}$ and increasing the resonator and coupling capacitance in order to keep p, ω, and Q constant. Consequently, these constraints set an upper limit on I_0 which can be utilized with the present design of microstrip resonators. Increasing I_0 by a factor of 3.3

($I_0 = 10\,\mu A$), for instance, would increase P_{max} by 10 dB but would also require decreasing the characteristic impedance to 15 Ω. In that case, it might be beneficial to replace the transmission-line resonators with planar capacitors and semi-lumped inductors.[6,11]

The numerous practical properties of this ultra-low added noise amplifier makes it suitable for the purpose of quantum nondemolition readout of superconducting qubits[23] which in turn leads to observation of quantum jumps[24] and quantum feedback.

[1]R. F. Bradley, Nucl. Phys. B **72**, 137 (1999).
[2]L. Roschier, P. Hakonen, K. Bladh, P. Delsing, K. W. Lehnert, L. Spietz, and R. J. Schoelkopf, J. Appl. Phys. **95**, 1274 (2004).
[3]K. Segall, K. W. Lehnert, T. R. Stevenson, R. J. Schoelkopf, P. Wahlgren, A. Aassime, and P. Delsing, Appl. Phys. Lett. **81**, 4859 (2002).
[4]D. Kinion and J. Clarke, Appl. Phys. Lett. **92**, 172503 (2008).
[5]M.-O. André, M. Mück, J. Clarke, J. Gail, and C. Heiden, Appl. Phys. Lett. **75**, 698 (1999).
[6]M. Hatridge, R. Vijay, D. H. Slichter, J. Clarke, and I. Siddiqi, Phys. Rev. B **83**, 134501 (2011).
[7]E. M. Levenson-Falk, R. Vijay, and I. Siddiqi, Appl. Phys. Lett. **98**, 123115 (2011).
[8]O. Astafiev, A. A. Abdumalikov, Jr., A. M. Zagoskin, Yu. A. Pashkin, Y. Nakamura, and J. S. Tsai, Phys. Rev. Lett. **104**, 183603 (2010).
[9]B. Yurke, L. R. Corruccini, P. G. Kaminsky, L. W. Rupp, A. D. Smith, A. H. Silver, R. W. Simon, and E. A. Whittaker, Phys. Rev. A **39**, 2519 (1989).
[10]R. Movshovich, B. Yurke, P. G. Kaminsky, A. D. Smith, A. H. Silver, R. W. Simon, and M. V. Schneider, Phys. Rev. Lett. **65**, 1419 (1990).
[11]I. Siddiqi, R. Vijay, F. Pierre, C. M. Wilson, M. Metcalfe, C. Rigetti, L. Frunzio, and M. H. Devoret, Phys. Rev. Lett. **93**, 207002 (2004).
[12]L. Spietz, K. Irwin, and J. Aumentado, Appl. Phys. Lett. **93**, 082506 (2008).
[13]L. Spietz, K. Irwin, M. Lee, and J. Aumentado, Appl. Phys. Lett. **97**, 142502 (2010).
[14]B. Abdo, O. Suchoi, E. Segev, O. Shtempluck, M. Blencowe, and E. Buks, Europhys. Lett. **85**, 68001 (2009).
[15]M. A. Castellanos-Beltran, K. D. Irwin, G. C. Hilton, L. R. Vale, and K. W. Lehnert, Nat. Phys. **4**, 928 (2008).
[16]M. A. Castellanos-Beltran and K. W. Lehnert, Appl. Phys. Lett. **91**, 083509 (2007).
[17]T. Yamamoto, K. Inomata, M. Watanabe, K. Matsuba, T. Miyazaki, W. D. Oliver, Y. Nakamura, and J. S. Tsai, Appl. Phys. Lett. **93**, 042510 (2008).
[18]N. Bergeal, F. Schackert, M. Metcalfe, R. Vijay, V. E. Manucharyan, L. Frunzio, D. E. Prober, R. J. Schoelkopf, S. M. Girvin, and M. H. Devoret, Nature **465**, 64 (2010).
[19]N. Bergeal, R. Vijay, V. E. Manucharyan, I. Siddiqi, R. J. Schoelkopf, S. M. Girvin, and M. H. Devoret, Nat. Phys. **6**, 296 (2010).
[20]C. M. Caves, Phys. Rev. D **26**, 1817 (1982).
[21]B. Abdo, A. Kamal, and M. H. Devoret, "Non-degenerate, 3-wave mixing with Josephson junction" (unpublished).
[22]V. E. Manucharyan, J. Koch, L. I. Glazman, and M. H. Devoret, Science **326**, 113 (2009).
[23]J. Gambetta, W. A. Braff, A. Wallraff, S. M. Girvin, and R. J. Schoelkopf, Phys. Rev. A **76**, 012325 (2007).
[24]R. Vijay, D. H. Slichter, and I. Siddiqi, Phys. Rev. Lett. **106**, 110502 (2011).